

Model-dependence of the CO₂ threshold for melting the hard Snowball Earth

Y. Hu¹, J. Yang¹, F. Ding¹, and W. R. Peltier²

¹Laboratory for Climate and Ocean-Atmosphere Studies, Dept. of Atmospheric and Oceanic Sciences, School of Physics, Peking University, 100871, Beijing, China

²Department of Physics, University of Toronto, 60 St. George Street, M5S 1A7, Toronto, Ontario, Canada

Received: 20 June 2010 – Published in *Clim. Past Discuss.*: 12 July 2010

Revised: 11 December 2010 – Accepted: 5 January 2011 – Published: 10 January 2011

Abstract. One of the critical issues of the Snowball Earth hypothesis is the CO₂ threshold for triggering the deglaciation. Using Community Atmospheric Model version 3.0 (CAM3), we study the problem for the CO₂ threshold. Our simulations show large differences from previous results (e.g. Pierrehumbert, 2004, 2005; Le Hir et al., 2007). At 0.2 bars of CO₂, the January maximum near-surface temperature is about 268 K, about 13 K higher than that in Pierrehumbert (2004, 2005), but lower than the value of 270 K for 0.1 bar of CO₂ in Le Hir et al. (2007). It is found that the difference of simulation results is mainly due to model sensitivity of greenhouse effect and longwave cloud forcing to increasing CO₂. At 0.2 bars of CO₂, CAM3 yields 117 Wm⁻² of clear-sky greenhouse effect and 32 Wm⁻² of longwave cloud forcing, versus only about 77 Wm⁻² and 10.5 Wm⁻² in Pierrehumbert (2004, 2005), respectively. CAM3 has comparable clear-sky greenhouse effect to that in Le Hir et al. (2007), but lower longwave cloud forcing. CAM3 also produces much stronger Hadley cells than that in Pierrehumbert (2005).

Effects of pressure broadening and collision-induced absorption are also studied using a radiative-convective model and CAM3. Both effects substantially increase surface temperature and thus lower the CO₂ threshold. The radiative-convective model yields a CO₂ threshold of about 0.21 bars with surface albedo of 0.663. Without considering the effects of pressure broadening and collision-induced absorption, CAM3 yields an approximate CO₂ threshold of about 1.0 bar for surface albedo of about 0.6. However, the threshold is lowered to 0.38 bars as both effects are considered.

1 Introduction

The Snowball Earth hypothesis is probably one of the most intriguing and fundamental problems in paleoclimate research in the past 10 years and received intensive debate (Kirschvink, 1992; Hoffman et al., 1998; Hoffman and Schrag, 2002). One of the important issues in Snowball Earth studies is the threshold of CO₂ concentration to rescue Earth from global glaciations (Pierrehumbert, 2004, 2005). According to the Snowball Earth hypothesis, the Snowball Earth was deglaciated by strong greenhouse effect due to high-level CO₂, which was accumulated due to volcanic eruptions over time scale of tens of millions of years when weathering reactions between CO₂ and surface rocks were cut off by snow-ice coverage.

The CO₂ threshold was estimated by simulation studies with both energy balance models (EBMs) and general circulation models (GCMs). EBMs yielded a wide range of values (Caldeira and Kasting, 1992; Hyde et al., 2000; Tajika, 2003). As commented by Pierrehumbert (2005), these different values would converge to about 0.2 ~ 0.3 bars of CO₂ as consistent conditions, such as surface albedo, cloud forcing and meridional heat-diffusivity, are considered. GCMs have more realistic dynamical and physical processes compared with EBMs and would provide more reliable results. However, GCM simulations also yielded different CO₂ thresholds. Using the fast oceanic atmospheric model (FOAM), Pierrehumbert (2004, 2005) found that even for 0.2 bars of CO₂ the annual-mean surface temperature at the equator is 30 K short of the melting point, suggesting that increasing CO₂ alone would be very difficult to melt the hard Snowball Earth, and that other mechanisms or feedback processes are needed. Indeed, Abbot and Pierrehumbert (2010) and Le Hir et al. (2010) showed that the CO₂ level required can be much lower (e.g., 0.01 ~ 0.1 bar) if a volcanic dust layer forms on the tropical surface. The dust layer would have



Correspondence to: Y. Hu
(yyhu@pku.edu.cn)

lowered surface albedo in the tropics, so that deglaciation can be triggered at lower CO₂ levels. Using a different atmospheric GCM (LMDz), Le Hir et al. (2007) reported that the hard Snowball Earth can be melted at 0.45 bars of CO₂. They showed that the major difference from FOAM simulation results is due to much stronger longwave cloud forcing in LMDz (Hereafter, Pierrehumbert (2004, 2005) and Le Hir et al. (2007) are also referred as FOAM and LMDz, respectively). The diversity of GCM simulations suggests that the CO₂ threshold is model dependent, as pointed out by Pierrehumbert (2005). In the present study, we report different simulation results of the CO₂ threshold from these previous GCM simulations. We also show that the differences are not only reflected in radiation, thermodynamics and cloud physics, but also in atmospheric dynamics, such as the Hadley circulation.

So far, both EBM and GCM models predicted that at least a few tenths of 1 bar of CO₂ is required to deglaciate the hard Snowball Earth. As CO₂ concentration reaches such a high level, the contribution of CO₂ partial pressure to total surface pressure cannot be neglected (Kasting, personal communication, 2010). The increase in total surface pressure increases absorption of greenhouse gases in the infrared region, which causes stronger greenhouse effect and increases surface temperature. This is because high pressure leads to more frequent collisions of air molecules, which broadens absorption lines and causes gases absorbing over a broader range of spectral lines in the infrared region. As a result, pressure broadening would lower the CO₂ threshold. The effects of pressure broadening and collision-induced absorption of greenhouse gases have not been considered in previous GCM simulations. Abbot and Pierrehumbert (2010) have argued that 0.1 or 0.2 bars of CO₂ might not increase the total surface pressure very much for the Snowball Earth period because atmospheric oxygen probably had a partial pressure of 0.15 bars lower than present levels according to Holland et al. (2006) and Canfield et al. (2007). Nevertheless, it is interesting to see how important the effect of pressure broadening on surface temperature and the CO₂ threshold. Therefore, in the present paper we will also examine the effect with a radiative-convective model and a GCM.

2 Models and experiments

The model used here is the CAM3 developed by the National Center for Atmospheric Research (Collins et al., 2004). It has a horizontal resolution of approximately $2.8^\circ \times 2.8^\circ$ in latitude and longitude and 26 vertical levels from the surface to approximately 2.0 hPa. CAM3 includes a thermodynamic sea-ice model, similar to the Community Sea Ice Model (Briegleb et al., 2004), with which snow depth, surface temperature, surface albedo, and energy fluxes between ice and overlying atmosphere can be predicted, while ice thickness and ice fractional coverage are both prescribed by

keeping ice-surface temperature below -1.8°C (271.35 K) (the model melting point of water). Below the model melting point, ice surface temperature varies, depending on energy budget over the surface. The ice prescription here is similar to that in Le Hir et al. (2007).

To simulate a hard Snowball Earth, we prescribe an ocean covered by fixed sea ice with thickness of 20 m. An idealized rectangular supercontinent is centered at the equator as in Pierrehumbert (2004, 2005) and Poulsen et al. (2001). Sea ice is covered by a snow layer with initial depth of 1 meter (liquid water equivalent). Snow depth varies with time. Solar luminosity is 94% of the present value. Eccentricity, obliquity, and rotation rate are all defined as present values. We use the same albedo values as Pierrehumbert (2005), that is, snow albedo is 0.9 and 0.6 for visible and near-infrared radiation, respectively. The sea-ice albedo is 0.5, independent of wavelength (Sea ice albedo in Pierrehumbert (2004, 2005) was 0.7. See Abbot and Pierrehumbert (2010) for detailed explanation). Various CO₂ levels have been set: 100, 400, 1600, 12 800 ppmv, 0.1, and 0.2 bars, same as Pierrehumbert (2004, 2005).

It is worth pointing out that the atmospheric component of FOAM used by Pierrehumbert (2004, 2005) is derived from CCM3, i.e., one of the previous versions of CAM3. CAM3 has several significant improvements in physical parameterizations relative to CCM3 (Collins et al., 2004), including revised cloud and precipitation parameterizations with prognostic formulations for the partitioning of cloud water between liquid and ice phases (Boville et al., 2006), updated radiation schemes for water vapor absorption in visible and infrared regions (Collins et al., 2002; Collins et al., 2006). As a result of these changes, CAM3 has a warmer, moister and more stable troposphere, and major features of temperature, water vapor, cloud and precipitation in CAM3 are more consistent with observational estimates compared with that in CCM3 (Hack et al., 2006). As shown below, these improvements cause significant differences in Snowball-Earth simulations. The results here will be compared with that in FOAM and LMDz to show model dependences.

To demonstrate effects of pressure broadening and collision-induced absorption for high CO₂ concentration, we use a radiative-convective model. This model was originally developed by Kasting et al. (1984a, b) for simulating dense planetary atmospheres with high levels of CO₂, and was later modified by Toon et al. (1989), Pavlov et al. (2000), Mischna et al. (2000), and others. The model takes into account effects of collision-induced absorption of CO₂, pressure-induced broadening of CO₂ and H₂O absorption, and Rayleigh scattering by CO₂. It has been used for radiation transfer and surface temperature simulations for the early Earth atmosphere that likely had very high levels of CO₂ (Kasting and Ackerman, 1986). The model has 38 spectral intervals in the visible- and near-infrared radiation (IR) and 55 spectral intervals in the thermal-IR. Infrared absorption by CO₂ and water vapor is calculated from the Air

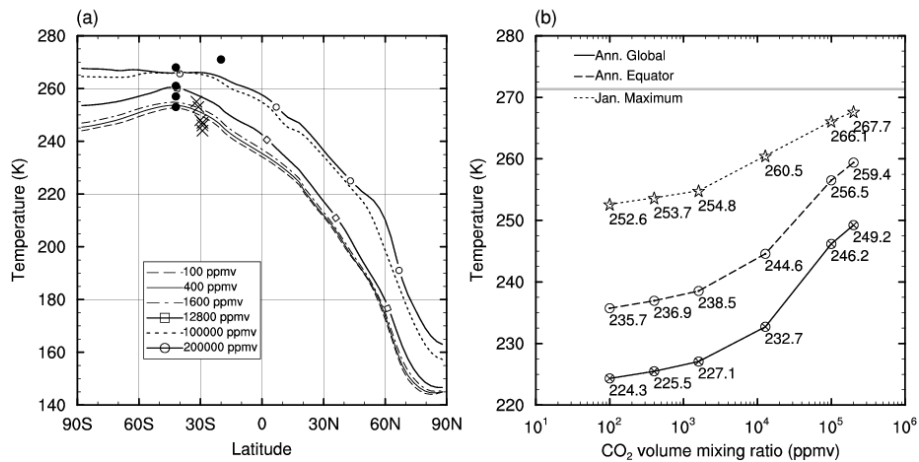


Fig. 1. (a) January zonal-mean air temperatures at the bottom model level for various CO₂ levels. Only sea-ice grid points are used in computing zonal-mean temperatures. (b) January zonal-mean maximum, equatorial annual-mean, and global annual-mean near-surface temperatures as a function of CO₂ levels. Note that the CO₂ volume mixing ratio here is based on the assumption of constant surface pressure of 1 bar. In Figure 1a, black dots from the bottom to top denote the maximum near-surface temperatures and their latitudes in LMDz, corresponding to 100, 330, 1600, 12800 ppmv, and 0.1 bar, respectively, and crosses indicate the maximum near-surface temperatures and their latitudes in FOAM, corresponding to 100, 400, 1600, 12 800 ppmv, 0.1, and 0.2 bars, respectively.

Force Geophysical Laboratory tape. Detailed description of the model can be found at <http://vpl.astro.washington.edu/sci/AntiModels/models09.html>. Hereafter, the model is denoted as Kasting's model.

3 Results

Figure 1a shows January zonal-mean air temperatures at the lowest model level (T_{BOT}) for various CO₂ levels. While the bulk meridional temperature structures are similar to that in FOAM, they show much stronger hemispheric temperature contrast between summer and winter hemispheres. For 100 ppmv of CO₂, the maximum temperature in the summer hemisphere (Southern Hemisphere) is about 253 K, which is close to that in LMDz, but about 5 K higher than that in FOAM. The maximum temperature is located at about 45° S, similar to that in LMDz, but more poleward than in FOAM. The lowest temperature of about 145 K is at the winter pole, which is about 20 K lower than that in FOAM, but 10 K higher than that in LMDz. As CO₂ level increases, the T_{BOT} increase is greater than in FOAM. At 0.2 bars of CO₂, the maximum T_{BOT} is about 268 K, about 5 K short of the freezing point. In contrast, FOAM yields a January maximum T_{BOT} of 255 K, and LMDz gives a value of 270 K for 0.1 bar of CO₂.

Figure 1b shows January maximum, global and annual mean, and annual-mean equatorial near-surface temperatures as a function of CO₂ levels. The temperatures show non-linear relationship with the logarithm of CO₂ concentration. At low levels of CO₂ (100–1600 ppmv), each quadrupling of CO₂ causes temperatures increased by about 1.1–1.4 K,

somehow less than the 2 K increase in FOAM. However, temperature increases become much greater as CO₂ level gets higher. Especially, for CO₂ levels from 12 800 ppmv to 0.1 bar, the equatorial annual-mean temperature is increased by about 12 K, equivalent to 4.0 K for each doubling of CO₂. As CO₂ increases from 0.1 to 0.2 bars, temperature increasing slows again, increasing by about 3 K. This is probably because of the sea-ice prescription that keeps ice-surface temperature below -1.8°C (271.35 K). Indeed, further increasing CO₂ results in T_{BOT} asymptoting to 271.35 K. If the equatorial annual-mean temperature of 273 K is considered as the standard for triggering the deglaciation of the Snowball Earth, as suggested by Pierrehumbert (2004, 2005), our simulations suggest that the CO₂ threshold would be close to 1.0 bar of CO₂ for the increasing rate of 4 K for each doubling CO₂. This estimated threshold is higher than that in LMDz (0.45 bars), but lower than that in FOAM.

A question is what cause different model sensitivities of near-surface temperatures to increasing CO₂? This can be demonstrated by evaluating the clear-sky greenhouse effect and longwave cloud forcing, by following Pierrehumbert (2004, 2005). Figure 2a shows the clear-sky greenhouse effect in January for various levels of CO₂. At 100 ppmv of CO₂, the maximum clear-sky greenhouse effect is about 50 Wm^{-2} . It is close to that in LMDz, but about 20 Wm^{-2} higher than in FOAM. As CO₂ increases to 0.1 bar, the maximum clear-sky greenhouse effect is up to 110 Wm^{-2} . It is about 5 and 45 Wm^{-2} higher than that in LMDz and FOAM, respectively. The stronger clear-sky greenhouse effect is presumably due to the improvement in radiation scheme for water vapor in CAM3, which increases the near-infrared absorption by water vapor and leads to a warmer and moister

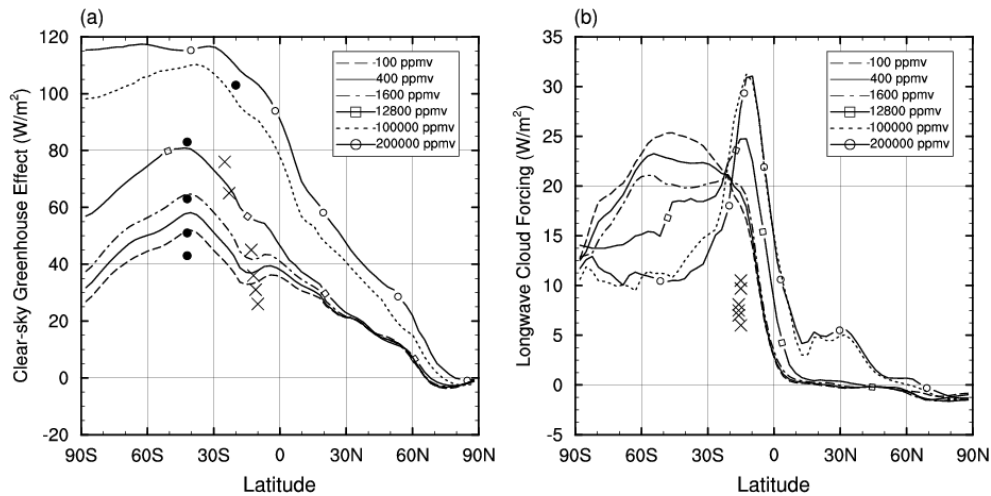


Fig. 2. January zonal-mean clear-sky greenhouse effect (a) and longwave cloud forcing (b) for various CO₂ levels. In Fig. 2a, black dots from the bottom to top denote the maximum clear-sky greenhouse effects and their latitudes in LMDz, corresponding to 100, 330, 1600, 12 800 ppmv, and 0.1 bar, respectively, and crosses indicate the maximum clear-sky greenhouse effects and their latitudes in FOAM, corresponding to 100, 400, 1600, 12 800 ppmv, 0.1, and 0.2 bars, respectively. Crosses in Fig. 2b marks the maximum longwave cloud forcing for various CO₂ levels in FOAM.

atmosphere (Collins et al., 2006). Increasing water vapor in the atmosphere consequently causes a stronger greenhouse effect. The location of the maximum clear-sky greenhouse effect also shows different meridional shifts from that in FOAM as CO₂ increases. It shifts equatorward from about 45° S for 100 ppmv CO₂ to about 30° S for 0.2 bars of CO₂. Such a shift is consistent with that in LMDz, but opposite to that in FOAM.

For the cold Snowball Earth condition, clouds exist mainly in the form of ice particles and thus have greenhouse effect, as pointed out by Pierrehumbert (2004, 2005). In FOAM, longwave cloud forcing is about 6 Wm⁻² for 100 ppmv of CO₂ and about 10.5 Wm⁻² for 0.2 bars of CO₂. In contrast, CAM3 has a much stronger longwave cloud forcing. Figure 2b shows longwave cloud forcing in January for various levels of CO₂. Unlike that in FOAM, the maximum longwave cloud forcing is located in middle latitudes of the summer hemisphere for low levels of CO₂, rather than around 12° S, and the maximum cloud forcing at middle latitudes decreases with CO₂ levels. We will address this phenomenon later.

Around 12° S, longwave cloud forcing increases with CO₂ levels. This is because increasing CO₂ warms the tropical surface, which leads to stronger upward motion associated with the Hadley circulation. Thus, more water vapor is transported into the atmosphere, causing more ice clouds and stronger greenhouse effect. For 100 ppmv, the maximum cloud forcing is about 26 Wm⁻², about 20 Wm⁻² higher than in FOAM. For 0.2 bars of CO₂, the cloud forcing is up to 32 Wm⁻², about 21.5 Wm⁻² higher than the FOAM value. The longwave cloud forcing in CAM3 is higher than in FOAM. However, it is lower than that in

LMDz. For 330 ppmv of CO₂, the maximum cloud forcing is 50 Wm⁻² in LMDz, which is twice larger than the 23 Wm⁻² for 400 ppmv of CO₂ in CAM3. The above results demonstrate that the higher near-surface temperatures in CAM3 than in FOAM for the same level of CO₂ is because both clear-sky greenhouse effect and longwave cloud forcing are much stronger in CAM3.

The decrease in maximum longwave cloud forcing at the summer-hemisphere middle latitudes can be addressed with Fig. 3. At 100 ppmv of CO₂, a cloud layer is located between 900 and 400 hPa (Fig. 3a) because relative humidity (RH) in this layer is above 80%, which is the threshold for cloud formation in CAM3 (Collins et al., 2004). As CO₂ level increases, the layer with RH greater than 80% is lifted to higher altitudes. For example, as CO₂ is up to 0.2 bars, such a layer is between 500 and 300 hPa. It appears that tropospheric warming due to increasing CO₂ causes reduction of saturation at lower tropospheric levels at the summer-hemisphere middle latitudes. Figure 3b shows vertical distribution of cloud fractions corresponding to Fig. 3a. One can find that large amount of clouds exists in almost all the troposphere for 100 ppmv of CO₂, and that the cloud layer is lifted to between 500 and 300 hPa as CO₂ is up to 0.2 bars. The rising of the cloud layer has two opposite effects on longwave cloud forcing. First, ice clouds at higher levels have stronger greenhouse effect since clouds emit less outgoing infrared radiation (OLR) at lower temperatures. Second, the rising of cloud layer causes less cloud formation because water vapor concentration decreases with altitudes (Fig. 3c), which would reduce greenhouse effect. It appears that the latter is dominant, which causes the decrease in longwave cloud forcing at middle latitudes of the summer hemisphere.

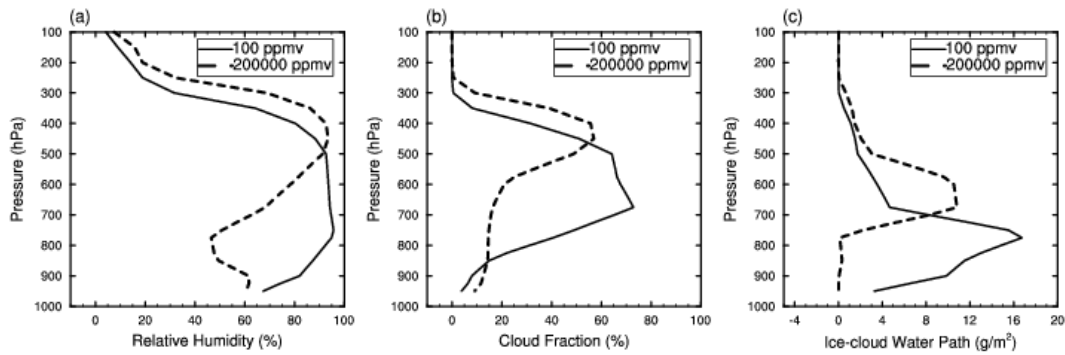


Fig. 3. Vertical distributions of relative humidity (a), cloud fraction (b), and ice-cloud water path (c), averaged between 30° S and 60° S.

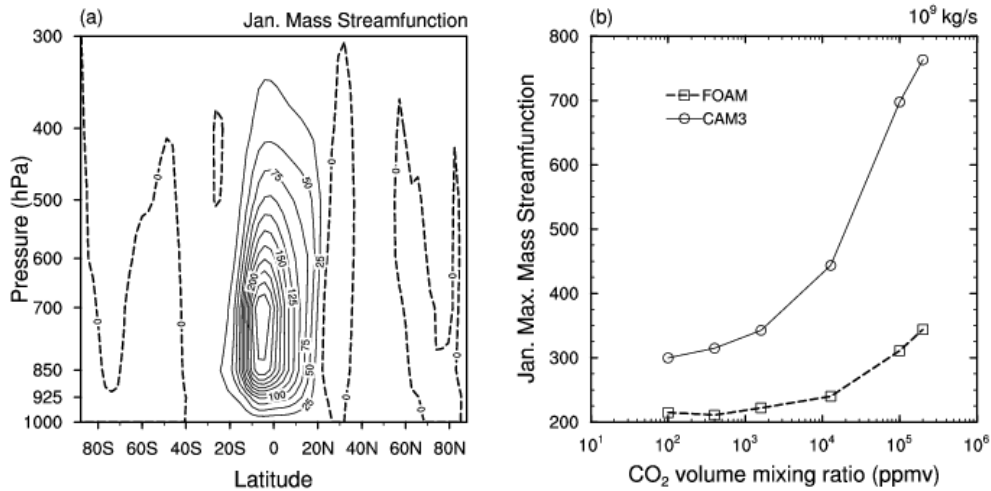


Fig. 4. (a) January meridional mass streamfunction for 100 ppmv of CO₂. Contour interval is $25 \times 10^9 \text{ Kgs}^{-1}$. (b) January maximum mass streamfunctions as a function of CO₂ level.

Model dependence is not only reflected in the physics part of simulations but also in atmospheric dynamics. Figure 4a shows the meridional mass streamfunction in January for 100 ppmv of CO₂. The Hadley circulation has similar horizontal extent as in FOAM, but shallower in depth. A significant difference from that in FOAM is that the Hadley circulation in CAM3 is much stronger. The maximum mass streamfunction in Fig. 4a is $300 \times 10^9 \text{ kgs}^{-1}$, vs. $215 \times 10^9 \text{ kgs}^{-1}$ in FOAM. Detailed comparison of the maximum mass streamfunction between CAM3 and FOAM is shown in Fig. 4b. In both models, the maximum mass streamfunction nonlinearly increases with the logarithm of CO₂ concentration, with much greater increasing in CAM3. At 0.2 bars of CO₂, the maximum streamfunction is about $760 \times 10^9 \text{ kgs}^{-1}$, vs. $344 \times 10^9 \text{ kgs}^{-1}$ in FOAM. The difference is presumably due to the stronger equator-pole temperature contrast in CAM3 than in FOAM (about 90 K vs. 70 K) since it is considered a major factor in determining the intensity of the Hadley circulation (Held and Hou, 1980).

In the above simulations, the surface pressure (P_s) in the model remains constant, i.e., 1.0 bar, and the contribution of the partial pressure of CO₂ to the total pressure is not considered. However, as large amounts of CO₂ (e.g. a few tenth of 1 bar of CO₂) is added to the model, increase in total pressure cannot be neglected. Since CO₂ molecule weight is much larger than the average air molecule weight (44 versus 29 g/mol), total pressure increases rapidly with increasing CO₂ volume mixing ratio. Figure 5 illustrates total surface pressure as a function of CO₂ volume mixing ratio. As CO₂ volume mixing ratio is less than 0.01, it does not lead to large increase in the total pressure. However, total pressure increases rapidly as CO₂ mixing ratio is greater than 0.1. From Fig. 5, one can find that 0.1 and 0.2 of CO₂ volume mixing ratio correspond to about 1.17 and 1.38 bars of total surface pressure.

The increase in total pressure substantially enhances greenhouse warming, throughout pressure broadening of absorption lines and collision-induced absorption of CO₂ and water vapor in the infrared region (Kasting, personal

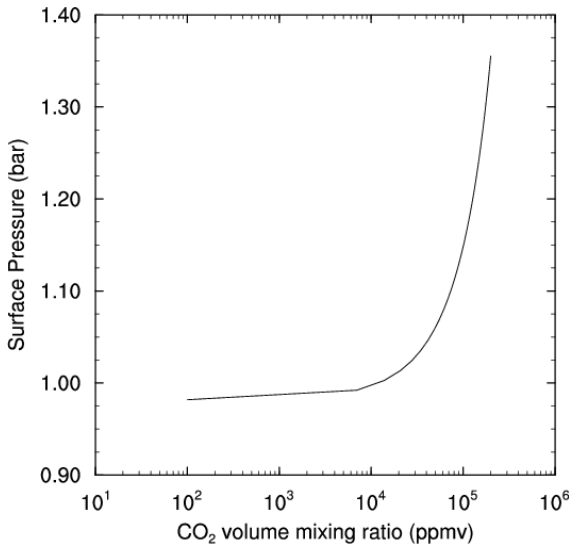


Fig. 5. Total surface pressure as a function of CO₂ volume mixing ratio.

communication, 2010). To show these effects of pressure broadening and collision-induced absorption of CO₂ and water vapor on surface temperatures, we first carry out simulations, using Kasting's radiative-convective model. Surface albedo is set to 0.663, same as that in Caldeira and Kasting (1992), and solar constant is 94% of the present value. Vertical distribution of RH is similar to that in Manabe and Wetherald (1967), with surface RH of 80%. The simulation results are shown in Fig. 6. As CO₂ volume mixing ratio is less than 0.01 (10 000 ppmv), the three lines overlap each other, indicating that both pressure broadening and collision-induced absorption cause little difference in surface temperature from that with 1 bar of surface pressure. For CO₂ volume mixing ratio higher than 0.01, the two kinds of effects start causing significant increasing of surface temperature, and the two effects become stronger with increasing CO₂ levels. For CO₂ volume mixing ratio of 0.1, 0.2, and 0.4 (the corresponding CO₂ partial pressure is 0.17, 0.38, and 1.0 bars, respectively), surface temperature increase due to pressure broadening is about 5, 9, and 49 K, respectively, and temperature increase due to collision-induced absorption is about 5, 9, and 10 K, respectively. It appears that the effect of pressure broadening is the dominant factor compared with that of collision-induced absorption as the CO₂ level is sufficiently high, while both effects are comparable for lower levels of CO₂. These indicate that pressure broadening and collision-induced absorption of CO₂ and water vapor can substantially reduce the CO₂ threshold. In Fig. 6, the CO₂ volume mixing ratio corresponding to the melting point is about 0.18, which is equivalent to about 0.33 bars of CO₂ by checking with Fig. 5. Note that results in Fig. 6 are approximately equivalent to the global and annual mean surface temperature. Considering that annual-mean equatorial

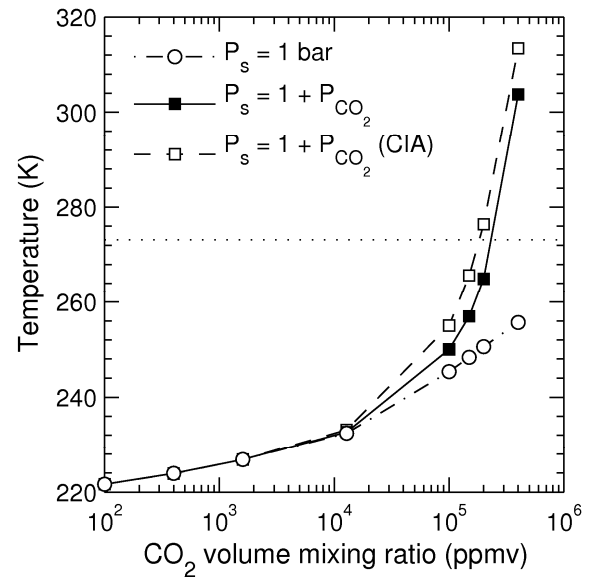


Fig. 6. Surface temperature as a function of CO₂ volume mixing ratio as the contribution of CO₂ partial pressure to total pressure is considered. Circle-dashed-dotted line: surface pressure is held constant, i.e., $P_s = 1.0$ bar, black-square-solid line: $P_s = 1.0 + P_{\text{CO}_2}$ partial pressure (P_{CO_2}), with only pressure broadening of absorption considered, and square-dashed line: $P_s = 1.0 + P_{\text{CO}_2}$, with both pressure broadening and collision-induced absorption (CIA) of CO₂ are considered. Here, the zenith angle is 60°.

temperature is usually about 10 K higher than global mean temperature (see Fig. 1b), CO₂ levels required for raising the equatorial temperature to the melting point would be lower than 0.33 bars. From Figs. 5 and 6, one can estimate that the CO₂ threshold for triggering equatorial deglaciation is about 0.21 bars.

The radiation module of CAM3 includes pressure broadening, but without collision-induced absorption. To examine the effect of pressure broadening in CAM3, we repeat the above simulations with considering the contribution of CO₂ partial pressure to total pressure in the model. Simulation results are shown in Fig. 7. Comparison of Fig. 7a with 1a demonstrates that January zonal-mean surface temperatures have no significant changes as CO₂ volume mixing ratio is less than 0.1. However, as CO₂ volume mixing ratio is up to 0.2, zonal-mean temperatures in the Northern Hemisphere (winter hemisphere) have large increases. At the North Pole, temperature is increased by about 46 K (from about 164 K to about 210 K), and at 30° N temperature is increased by about 10 K. In contrast, temperatures in the summer hemisphere show much weaker increase. It is because of the limit of sea-ice prescription, as mentioned before. Figure 7b shows global- and annual-mean, equatorial annual-mean, and January maximum surface temperatures as a function of CO₂ volume mixing ratio. For 0.2 of CO₂ volume mixing ratio, the temperatures are about 8, 6.7, and 3.2 K higher than that

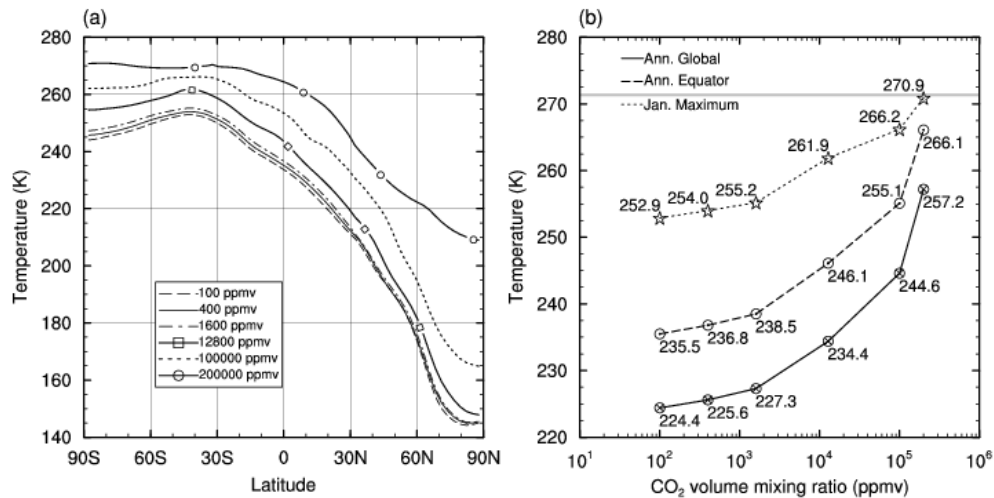


Fig. 7. Same as Fig. 1, except for that the contribution of CO₂ partial pressure to total pressure and the effect of pressure-broadening are considered.

in Figure 1b, respectively. The January maximum temperature has the smallest increase because the January maximum temperature in Figure 1b is already close to the model melting point. The global- and annual-mean surface temperature has the largest increase, mainly due to large temperature increases in the winter hemisphere. Note that for the same volume mixing ratio of 0.2 the partial pressure of CO₂ in Fig. 7 is nearly twice larger than that in Fig. 1b (0.38 vs. 0.2 bars), and CO₂ mass is increased by 0.38 times. Therefore, the increase in surface temperature from Fig. 1b to 7b is not only due to pressure broadening but also due to CO₂ mass increasing. Considering the rate of 3 K for CO₂ level from 0.1 bar to 0.2 bars as shown in Fig. 1b, the increase in CO₂ mass leads to temperature increase by about 1.1 K. Thus, in CAM3 the increase in equatorial annual-mean temperature due to pressure broadening is about 5.6 K. It is about half of that in Kasting's radiative-convective model. Assuming that collision-induced absorption causes the same magnitude of temperature increasing, the equatorial annual-mean surface temperature would be close to the melting point for CO₂ volume mixing ratio of 0.2. Thus, the CO₂ threshold estimated from CAM3 is about 0.38 bars, higher than that in Kasting's radiative-convective model.

4 Summary

We have re-examined the problem for the deglaciation of the hard Snowball Earth with CAM3. It is found that CAM3 yields higher near-surface temperatures than that in FOAM at same CO₂ levels. The higher temperature in CAM3 is because it generates much stronger clear-sky greenhouse effect and longwave cloud forcing. At 0.2 bars of CO₂, the clear-sky greenhouse effect and longwave cloud forcing are

117 Wm⁻² and 32 Wm⁻², respectively, versus 77 Wm⁻² and 10.5 Wm⁻² in FOAM. The clear-sky greenhouse effect in CAM3 is close to that in LMDz. However, the longwave cloud forcing in CAM3 is much lower than in LMDz, i.e., 23 Wm⁻² vs. 50 Wm⁻² for about 400 ppmv of CO₂. CAM3 also produces a much stronger Hadley cell in the winter hemisphere than in FOAM because it has larger temperature contrast between the equator and the winter hemisphere. All these suggest that simulation results of the CO₂ threshold for deglaciating the hard Snowball Earth are model dependent and have large uncertainty. It is similar to the model-dependent CO₂ threshold for Snowball Earth glaciation, as pointed out by Poulsen and Jacob (2004) who found that the CO₂ threshold for Snowball Earth formation is also dependent on model physics, such as clouds and sea ice.

The difference of the CO₂ threshold among the GCM simulations is mainly due to two factors: different surface albedo and parameterizations of cloud physics. In Pierrehumbert (2004) and (2005), the sea-ice albedo remains 0.7 by model default (Abbot and Pierrehumbert, 2010), and the global-mean surface albedo is about 0.664, whereas the global-mean surface albedo in CAM3 is about 0.60 for 0.2 bars of CO₂, largely due to snow melting. It suggests that for global average the surface receives about 20 Wm⁻² more solar radiation in CAM3 than in FOAM, which is nearly equal to the difference of longwave cloud forcing between CAM3 and FOAM. We would think that surface albedo in LMDz is also lower than in FOAM, although it was not reported in Le Hir et al. (2007). The lower surface albedo in CAM3 may also partly contribute to the stronger clear-sky greenhouse effect, throughout feedbacks. Lower surface albedo leads to higher surface temperature, causing more water vapor in the atmosphere, through sublimation. The increase in water vapor increases clear-sky greenhouse effect and hence

surface temperature. The increase in water vapor also increases ice clouds for the cold Snowball-Earth condition, which causes stronger positive cloud forcing.

We also studied the effects of pressure broadening and collision-induced absorption on the CO₂ threshold, using Kasting's radiative-convective model and CAM3. It is found that both effects increase surface temperature substantially as CO₂ volume mixing ratio is higher than 0.1. As both pressure broadening and collision-induced absorption are all considered, the CO₂ threshold in Kasting's model is about 0.21 bars with surface albedo of 0.663. The effect of pressure broadening in CAM3 is weaker than in Kasting's radiative-convective model. CAM3 yields a CO₂ threshold of about 0.38 bars for surface albedo of about 0.6 as both effects are considered. In contrast, the CO₂ threshold is close to 1.0 bar as pressure broadening and collision-induced absorption are not considered.

Acknowledgements. We are grateful to J. Kasting who encouraged us to carry out simulations with pressure broadening and showed us his unpublished results. We thank the other anonymous reviewer for helpful comments. This work is supported by the National Basic Research Program of China (973 Program, 2010CB428606), the National Natural Science Foundation of China under grants 40875042 and 41025018, and the Ministry of Education of China (20070001002). Part of the computations on which this paper is based was performed at the SciNet facility for High Performance Computation at the University of Toronto. SciNet is a component of the Compute Canada platform for HPC. J. Yang is partly supported by the Oversea Study Program for Graduate Students of the China Scholarship Council

Edited by: H. Renssen

References

- Abbot, D. S. and Pierrehumbert, R. T.: Mudball: Surface dust and snowball Earth deglaciation, *J. Geophys. Res.*, 115, D03104, doi:10.1029/2009JD012007, 2010.
- Boville, B. A., Rasch P. J., Hack J. J., and McCaa J. R.: Representation of clouds and precipitation processes in the Community Atmosphere Model version 3 (CAM3), *J. Climate*, 19, 2162–2183, 2006.
- Briegleb, B. P., Bitz, C. M., Hunke, E. C., Lipscomb, W. H., Holland, M. M., Schramm, J. L., and Moritz, R. E.: Scientific description of the sea ice component in the Community Climate System Model, Version Three. Technical Note, NCAR/TN-463.STR, National Center for Atmospheric Research, Boulder, Colorado, 78 pp., 2004.
- Caldeira, K. and Kasting, J. F.: Susceptibility of the early Earth to irreversible glaciation caused by carbon dioxide clouds, *Nature*, 359, 226–228, 1992.
- Canfield, D. E., Poulton, S. W., and Narbonne, G. M.: Late-Neoproterozoic deep-ocean oxygenation and the rise of animal life, *Science*, 315(5808), 92–95, 2007.
- Collins, W. D., Hackney, J. K., and Edwards, D. P.: An updated parameterization for infrared emission and absorption by water vapor in the National Center for Atmospheric Research Community Atmosphere Model, *J. Geophys. Res.*, 107(D22), 4664, doi:10.1029/2001JD001365, 2002.
- Collins, W. D., Rasch, P. J., Boville, B. A., Hack, J. J., McCaa, J. R., Williamson, D. L., Kiehl, J. T., Briegleb, B., Bitz, C., Lin, S.-J., Zhang, M., and Dai, Y.: Description of the NCAR Community Atmosphere Model: CAM3.0, Technical Note, NCAR/TN-464.STR, National Center for Atmospheric Research, Boulder, Colorado, 226 pp., available online at <http://www.cesm.ucar.edu/models/atm-cam>, 2004.
- Collins, W. D., Lee-Taylor J. M., Edwards D. P., and Francis G. L.: Effects of increased near-infrared absorption by water vapor on the climate system, *J. Geophys. Res.*, 111, D18109, doi:10.1029/2005JD006796, 2006.
- Hack, J. J., Caron, J. M., Yeager, S. G., Olson, K. W., Holland, M. M., Truesdale, J. E., and Rasch, P. J.: Simulation of the global hydrological cycle in the CCSM Community Atmosphere Model version 3 (CAM3): Mean features, *J. Climate*, 19, 2199–2221, 2006.
- Held, I. M. and Hou A. Y.: Nonlinear axially symmetric circulations in a nearly inviscid atmosphere, *J. Atmos. Sci.*, 37, 515–533, 1980.
- Hoffman, P. F., Kaufman A. J., Halverson G. P., and Schrag D. P.: A Neoproterozoic snowball Earth, *Science*, 281, 1342–1346, 1998.
- Hoffman, P. F. and Schrag D. P.: The snowball Earth hypothesis: Testing the limits of global change, *Terra Nova*, 14, 129–155, 2002.
- Holland H. D.: The oxygenation of the atmosphere and oceans, *Phil. Trans. R. Soc.*, B, 361, 903–915, 2006.
- Hyde, W. T., Crowley T. J., Baum S. K., and Peltier W. R.: Neoproterozoic “snowball Earth” simulations with a coupled climate/ice-sheet model, *Nature*, 405, 425–429, 2000.
- Kasting, J. F., Pollack, J. B., and Ackerman, T. P.: Response of Earth's atmosphere to increases in solar flux and implications for loss of water from Venus, *Icarus*, 57, 335–355, 1984a.
- Kasting, J. F., Pollack, J. B., and Crisp, D.: Effects of high CO₂ levels on surface temperature and atmospheric oxidation state of the early Earth, *J. Atmos. Chem.*, 1, 403–428, 1984b.
- Kasting, J. F. and Ackerman, T. P.: Climatic Consequences of Very High CO₂ Levels in Earth's Early Atmosphere, *Science*, 234, 1383–1385, 1986.
- Kirschvink, J. L.: Late Proterozoic low-latitude global glaciation: The snowball Earth, in *The Proterozoic Biosphere*, edited by: Schopf, J. W. and Klein, C., 51–52, Cambridge Univ. Press, New York., 1992.
- Le Hir, G., Ramstein, G., Donnadieu, Y., and Pierrehumbert, R. T.: Investigating plausible mechanisms to trigger a deglaciation from a hard snowball Earth, *C. Geoscience*, 339(3–4), 274–287, 2007.
- Le Hir, G., Donnadieu, Y., Krinner, G., and Ramstein, G.: Toward the snowball earth deglaciation, *Clim. Dyn.*, 35, 285–297, 2010.
- Manabe, S. and Wetherald, R. T.: Thermal equilibrium of the atmosphere with a given distribution of relative humidity, *J. Atmos. Sci.*, 24, 241–259, 1967.
- Mischna, M. A., Pavlov, A. A., and Kasting, J. F.: Influence of carbon dioxide clouds on early Martian climate, *Icarus*, 145, 546–554, 2000.
- Pavlov, A. A., Kasting, J. F., Brown, L. L., Rages, K. A., and Freedman, R.: Greenhouse warming by CH₄ in the atmosphere of early

- Earth, *J. Geophys. Res.*, 105, 11981–11990, 2000.
- Pierrehumbert, R. T.: High levels of atmospheric carbon dioxide necessary for the termination of global glaciation, *Nature*, 429, 646–649, 2004.
- Pierrehumbert, R. T.: Climate dynamics of a hard snowball Earth, *J. Geophys. Res.*, 110, D01111, doi:10.1029/2004JD005162, 2005.
- Poulsen, C. J., Pierrehumbert R. T., and Jacob R.: Impact of ocean dynamics on the simulation of the Neoproterozoic “snowball Earth”, *Geophys. Res. Lett.*, 28, 1575–1578, 2001.
- Poulsen, C. J. and Jacob, R.: Factors that inhibit Snowball Earth simulation, *Paleoceanography*, 19, PA4021, doi:10.1029/2004PA001056, 2004.
- Tajika, E.: Faint young Sun and the carbon cycle: Implication for the Proterozoic global glaciations, *Earth Planet. Sci. Lett.*, 214, 443–453, 2003.
- Toon, O. B., McKay, C. P., Ackerman, T. P., and Santhanam, K.: Rapid calculation of radiative heating rates and photodissociation rates in inhomogeneous multiple scattering atmospheres, *J. Geophys. Res.*, 94, 16287–16301, 1989.